

12.520 Lecture Notes 6

Possible cause of “weak” faults

- Preexisting fracture

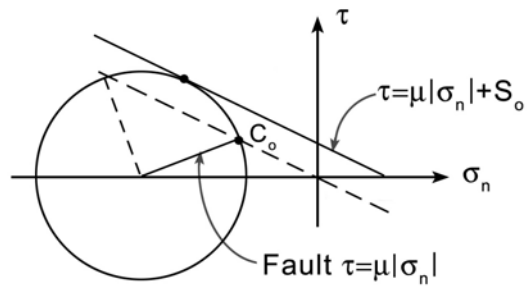


Fig. 6_1

- Clay \Rightarrow low μ

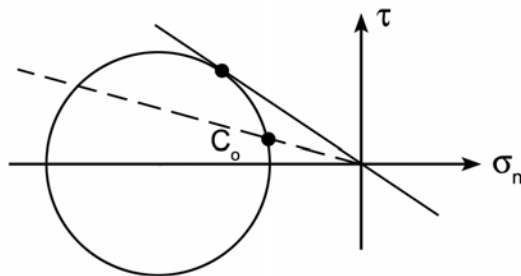


Fig. 6_2

- Pore fluid

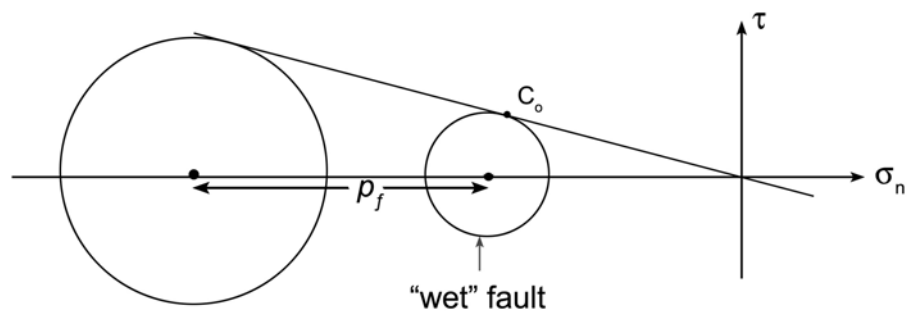


Fig. 6_3

How to get quantitative graphs? Make assumption!

Zoback et al example.

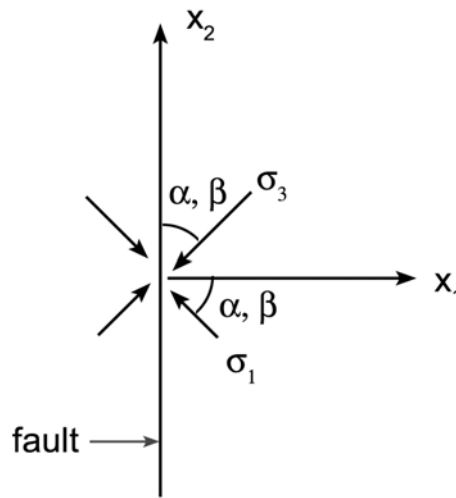


Fig. 6_4

Assume σ_c constant. $\tau_{fault} = c_0$.

Given β, c_0, σ_r get α .

Question: In far field, $\sigma_{12} = c_F$.

On fault $\sigma_{12} = c_0$.

$$\frac{\partial \sigma_{12}}{\partial x_1} > 0 \text{ -- How can this be?}$$

Another approach: Assume $\sigma_\tau \equiv c_0$, find σ_r given α .

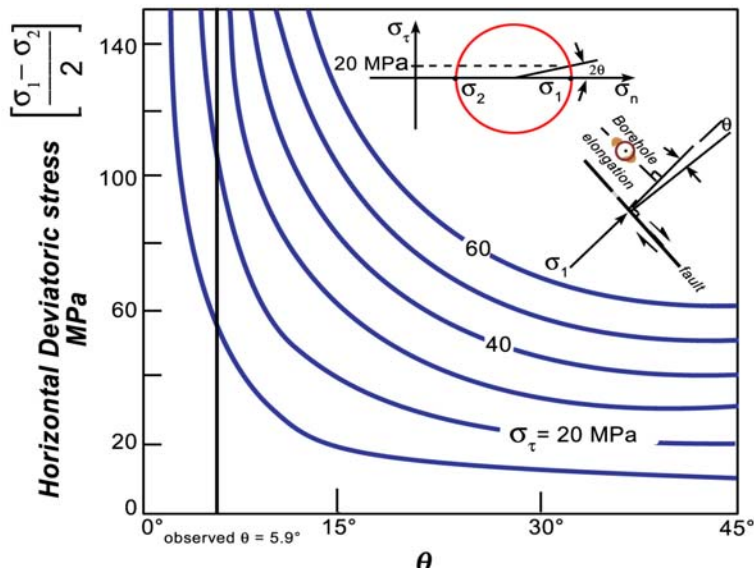


Fig. 6_5

Pore fluid pressure model of fault weakening

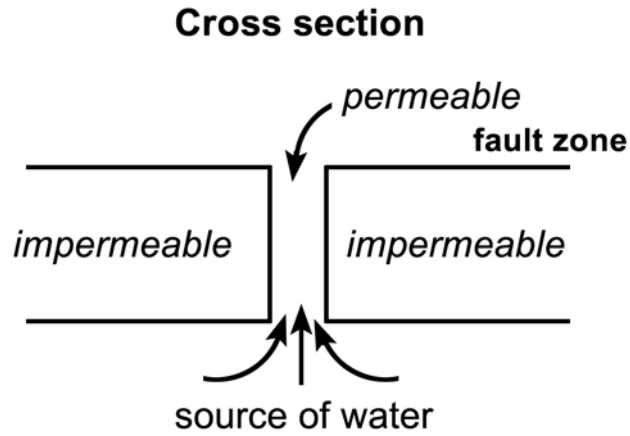


Fig. 6_6

Fault zone highly permeable

Darcy flow \approx heat flow
Permeability \approx conductivity
 $p \approx T$

Given source of water
High permeability \Rightarrow high p

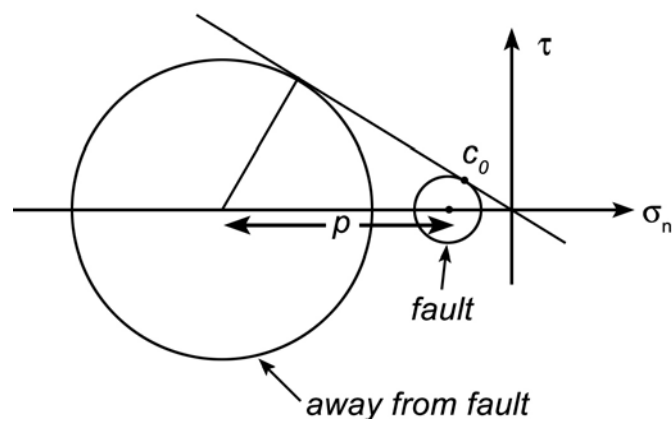


Fig. 6_7

Question:

- What are implications for stress direction in fault zone?
- Is low $\Delta\sigma$ in fault zone consistent with large $\Delta\sigma$ outside?

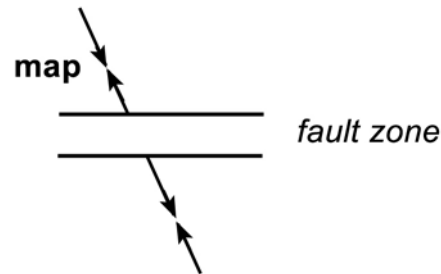


Fig. 6_8

Stress Rotation, after Zoback et al, 1987

The principal stress directions are observed to rotate in the vicinity of the San Andreas fault (SAF). In the far-field (e.g., Nevada), the maximum compressive stress is oriented at an angle to the fault trace $\beta \sim 55^\circ$. But in the near field, this angle, now called α , is close to 85° . (Note that this is the same as the angle between the least compressive stress and the normal to the fault plane, the angle conventionally used in Mohr circle analysis.)

Assume that in the far-field stress has $\sigma_I = -68$ MPa, σ_{II} (assumed vertical and lithostatic) = -136 MPa, and $\sigma_{III} = -204$ MPa. (What style of faulting would this cause?)

Assume that the fault has strength C_0 , so that σ_{12} becomes smaller approaching the fault. (How could this happen, given Newton's second law?).

Also assume that the normal stress across the fault maintains its far-field value (σ_{22} in the coordinate system fixed to the fault, as shown in the diagram). Assume that σ_c remains the same. (Does this agree with the style of faulting and the folding near the SAF?)

Then, from a Mohr's circle construction, it is straightforward to obtain a relation between α and β .

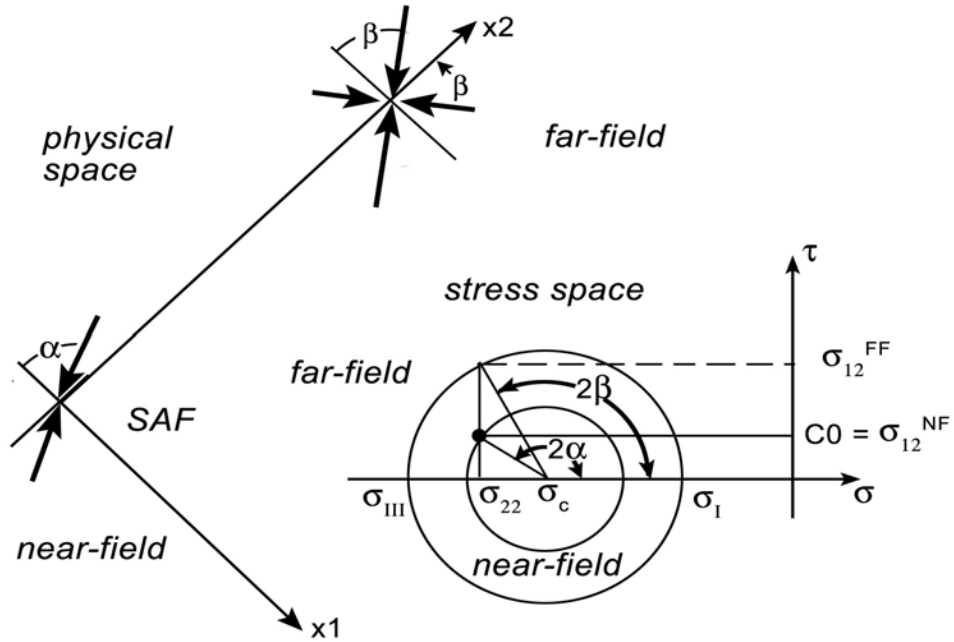
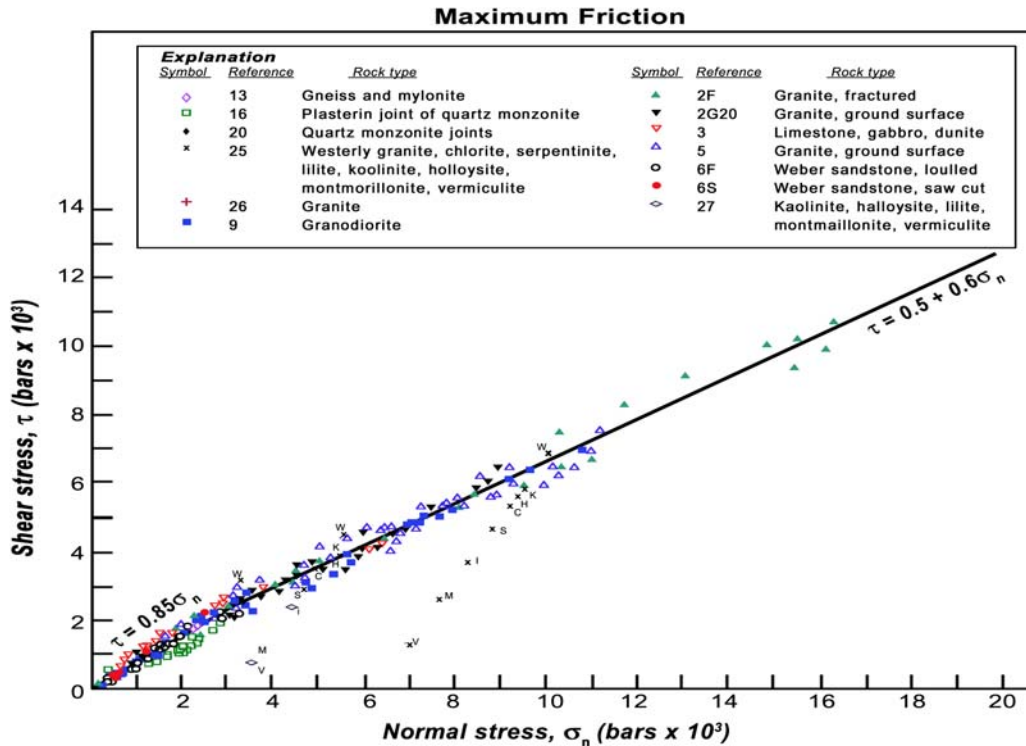


Fig. 6_9

The coefficients of friction, μ , for a wide variety of rocks, are comparable, in the range 0.6 – 0.9. The only rocks with low coefficients of friction are clays, which are not stable at the high pressures and temperatures characteristic of fault zones at depths of ~ 10 km where earthquakes nucleate.



Shear stress plotted as a function of normal stress at the maximum friction for a variety of rock types at normal stresses to 20kb.

data from Byerlee, **Pageoph**, 116, 1978

Fig. 6_10

Note: the Navier-Coulomb failure law, $|\tau| = \mu|\sigma| + \sigma_0$, is also sometimes written

$$|\tau| = \mu|\sigma| + S_0.$$

For rocks, $S_0 \sim 0.1 - 4$ kbars (10 - 400 MPa). How does this "breaking strength compare with the "frictional stress?"

Plot stress predicted for the initiation of faulting as a function of depth, assuming that σ is the lithostatic stress. (Recall that the "lithostatic stress gradient ~ 1 kbar/3 km.)

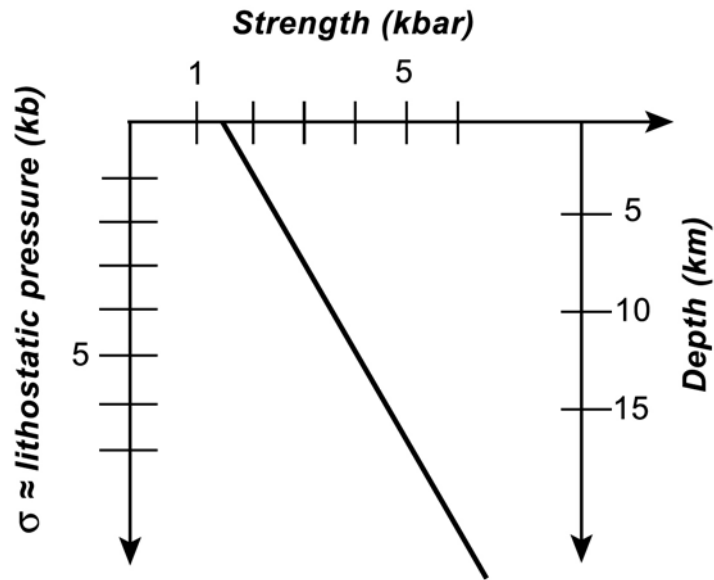


Fig. 6_11

So, if Byerlee's law is correct, and if the stress in the lithosphere is not too far from lithostatic, the shear stress on faults should be ~ 5 kbar at 15 km depth and about 250 kbar at 700 km depth.

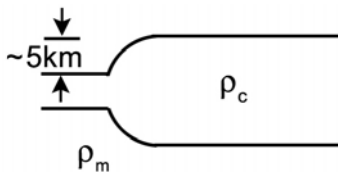


Fig. 6_12

How can we test this prediction?

- Model stresses associated with holding up mountains (e.g., Himalayas > 1.5 kbar)
- Stress drops associated with earthquakes (usually ~ 3 - 300 bars, very rarely > 1 kbar)
- Work available from convection (dynamic "engine," $< \sim 1$ kbar)
- Heat flow in fault zones (frictional heating rate $\sim \tau v \Rightarrow \tau \sim 100$ bars)

Big discrepancies here - a frontier region of geodynamics.

Important factor - the role of **pore fluid pressure** in faults.

Empirical results: For a pore fluid pressure p , the Navier-Coulomb failure law becomes:

$$|\tau| = \mu|\sigma+p| + S_0$$

(Note that because compressive pressure is positive, while compressive normal stress σ is negative, the pressure decreases the amplitude of the "effective normal stress" $|\sigma+p|$.)

Graphically:

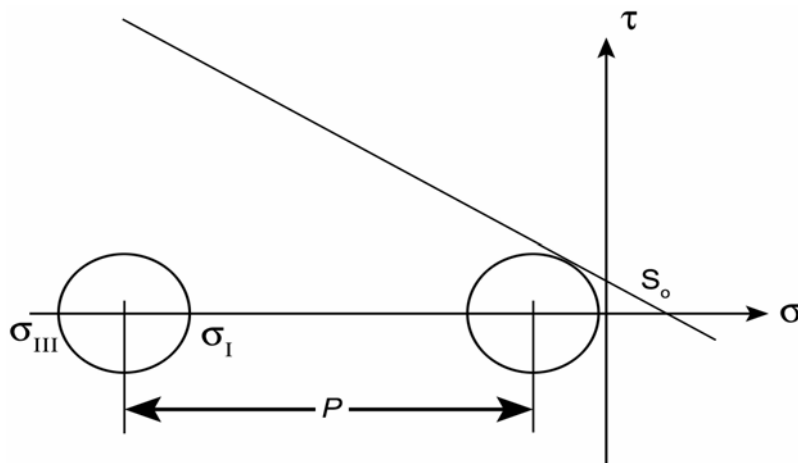


Fig. 6_13

A qualitative explanation of the effect of pore fluid pressure is that the the fluid helps to "support" some of the normal stress that is otherwise carried by solid grains. Consider a simple model of a continuum made up of dry sand. Let f_A represent the fraction of a surface area that is made up of solid grain contacts. Then for a macroscopic normal stress σ , the *average* (microscopic) normal stress at the solid grain contacts is σ/f_A , since the pore space in between can support no normal tractions. (Of course, in places the actual value will be much larger than the average value.) If Admonton's law applies to the

contacts, then the microscopic shear traction needed to cause failure is $\mu\sigma/f_A$, and the macroscopic shear traction is $\tau=\mu\sigma$.

If pore fluid pressure is now introduced, the pore fluid will support some of the macroscopic normal stress, leading to a decrease to the normal stress at the grain contacts.

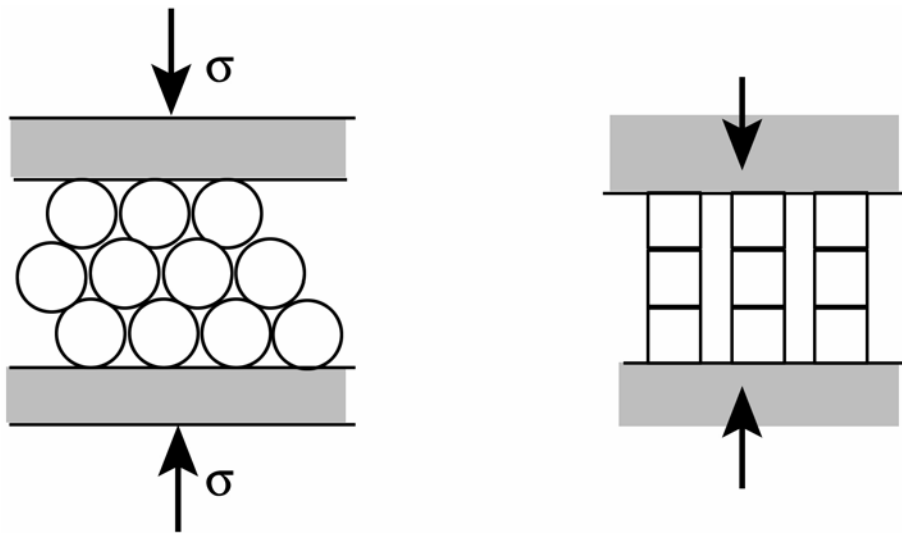


Fig. 6_14

Adding pore fluid pressure effectively "stretches" the σ_n axis, giving, effectively, a lower coefficient of friction (except that angles no longer work out!)

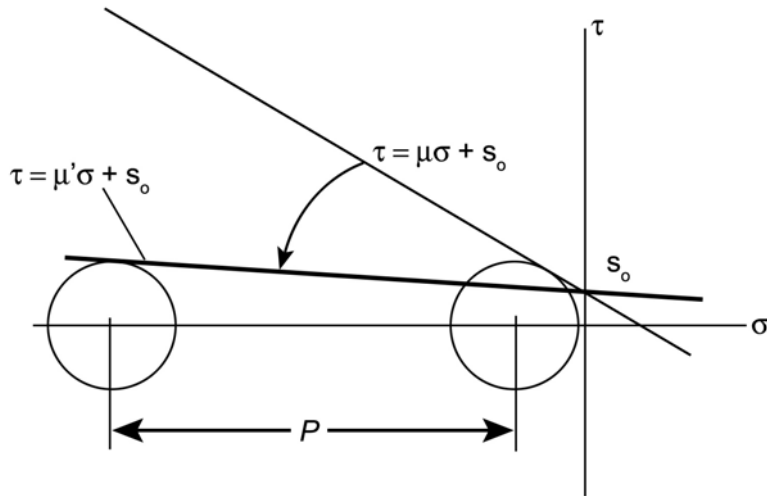


Fig. 6_15

An alternative explanation for deep earthquakes is that the failure envelope bends over at large σ_n .

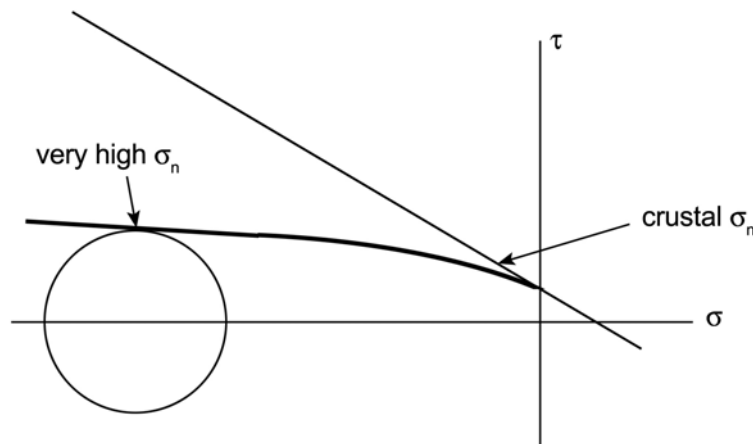


Fig. 6_16

Finally, let's consider a medium that is anisotropic – perhaps one which has a preexisting fracture at an angle θ to the least principal stress. (For a preexisting fracture, the strength $S_0 = 0$.) Then if the double angle 2θ is within the region shown, the rock will fail along the preexisting fracture.

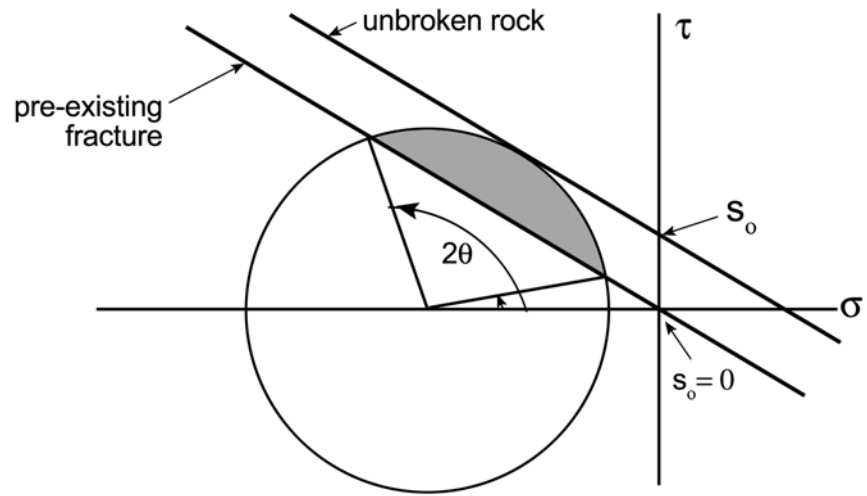


Fig. 6_17